

MICROWAVE IMAGING OF DIELECTRIC CYLINDERS USING LEVEL SET METHOD AND CONJUGATE GRADIENT ALGORITHM

K. Grayaa *

Syscom Laboratory, Engineer School of Tunis, University of Tunis El Manar, ESSTT, 5 Av Taha Hussen, Box 56, Bab Mnara, Tunis 1008, Tunisia

Abstract—In this paper, a level set method for shape reconstruction problems is considered. By measuring the scattered field, we tried to retrieve the localisation and permittivity of buried objects. The forward problem is solved by the method of moments. For solving the inverse problem, we adopt an evolution approach. Therefore, we introduce a level set technique which is flexible in handling complex shape changes. A conjugate gradient-based method is used in order to define iterative updates for the level set functions with the goal to minimize a given least squares data misfit functional. In particular, the proposed method is capable of creating new holes inside the design domain, which makes the final design independent of initial guess and reduces the probability of converging to a local minimum. Experimental results demonstrate the feasibility and effectiveness of the proposed technique.

1. INTRODUCTION

The microwave imaging has been extensively studied in the past years because of its various applications in many areas such as medicine [1, 2], biology [3], geophysics [4], and other sciences. In microwave tomography, the inverse scattering problem is solved to retrieve the complex permittivity profile of the object from the measured scattered field and applied incident field. This can be done with two different approaches, solving the nonlinear inverse problem or using different linear approximations, such as the Born or Rytov approximations. The linear approach is computationally

Received 2 December 2011, Accepted 9 February 2012, Scheduled 17 February 2012

* Corresponding author: Khaled Grayaa (khaled.grayaa@esstt.rnu.tn).

efficient and suitable for small objects with low contrast [5]. However, in many applications, the objects are large with high dielectric contrast, limiting the usability of the linear approximations. Therefore, more often different deterministic algorithms are applied to electromagnetic inverse scattering problem such as, the Newton–Kantorovich method [5, 6], modified gradient method [7] and distorted Born iterative method [5]. These methods represent the microwave imaging as a nonlinear optimization problem. The measured scattered field is iteratively compared with the computed field from the direct problem with the complex permittivity profile estimation and an applied incident field model. The major problem of these methods is the requirement of an accurate initial estimate profile for the object. To overcome these difficulties, others approaches based on genetic algorithms, particle swarm optimization and neural networks [8, 9] were developed for microwave imaging of buried objects.

In this paper, we propose an efficient scheme that uses a level set technique in conjunction with the conjugate gradient method to detect the location and shape of dielectric objects embedded in free space.

The level set method was investigated by Osher and Sethian for numerically tracking fronts and free boundaries [10]. Since then, it has found applications such as image processing [11], computer vision [12] and shape reconstruction [13, 14]. The level set shape reconstruction algorithm is capable of providing very good results even for low signal to noise ratio data. In addition, it can handle topological changes in an automatic way, which allows the reconstruction of multiple objects using a single initial guess.

In our work, the reconstruction of the permittivity profile of cylindrical objects in free space is solved by a controlled evolution of a level set function. This evolution is governed by a Hamilton–Jacobi type equation, whose velocity function has to be determined properly in order to minimize the data least squares misfit cost functional using a conjugate gradient-based scheme. A great advantage of using the proposed technique is the flexibility with which additional regularization term can be incorporated into the inversion scheme. Thus, the length of level set curves is added to the cost functional, as a regularization term, to stabilize the reconstruction process.

2. THE FORWARD PROBLEM

Let us consider two-dimensional (2-D) geometry as shown in Fig. 1.

The object with cross section Ω is assumed infinitely long (along the z -axis) and embedded in a homogenous space medium with a permittivity ε_{ext} .

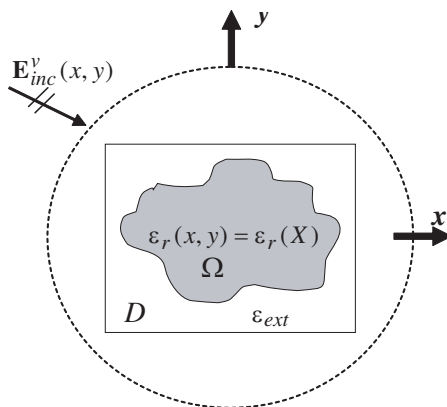


Figure 1. Geometric configuration of the 2-D scattering problem.

The material property of the object is characterized by the relative complex permittivity $\varepsilon_r(X)$.

The object domain is illuminated by a TM incident plane wave. The total electric field is a solution of the Helmholtz wave equation below:

$$\nabla \mathbf{E}(x, y) + k_0^2 \varepsilon_r(x, y) \mathbf{E}(x, y) = 0 \tag{1}$$

where k_0^2 denotes the wave number of the free space, and $\varepsilon_r(x, y)$ is the relative complex permittivity distribution in all space:

$$\varepsilon_r(x, y) = \begin{cases} \varepsilon_r(x, y), & (x, y) \in \Omega \\ \varepsilon_{ext}, & (x, y) \notin \Omega \end{cases} \tag{2}$$

The forward problem consists of computing the scattered field \mathbf{E}_s from the knowledge of permittivity profile and a particular incident field \mathbf{E}_{inc} . However, the tomography imaging objective is to find out an unknown permittivity distribution from measured scattered fields (data) and a given incident field. The electric field is a solution of the following reduced equation [8]:

$$\nabla \mathbf{E}(x, y) + k_0^2 \varepsilon_{ext} \mathbf{E}(x, y) = -k_0^2 q(x, y) \mathbf{E}(x, y), \tag{3}$$

where $q(x, y) = (\varepsilon_r(x, y) - \varepsilon_{ext})$ denotes the contrast function. When the object is illuminated by a set of V TM incident fields, the total electric field $\mathbf{E}^v(x, y)$, $v = 1 \dots V$, satisfies the following integral equation, which is also called the “state equation”:

$$\mathbf{E}^v(X) = \mathbf{E}_{inc}^v(X) + k_0^2 \iint_D g(X, X') q(X') E^v(X') dx' dy', \quad (X) \in D, \tag{4}$$

In (4), $g(x, y, x', y')$ is the Green's function given by:

$$g(x, y, x', y') = (j/4)H_0^{(1)}\left(k_0\sqrt{(x-x')^2 + (y-y')^2}\right),$$

Here $H_0^{(1)}$ is the Hankel function. The measurement domain S is formed by an arrangement of probing antennas located at M positions (x_m, y_m) , $m = 1, \dots, M$, and surrounding the object domain D . Let us use this equality: $\tilde{\mathbf{E}} = \tilde{\mathbf{E}}_s + \tilde{\mathbf{E}}_{inc}$, then for each excitation of index v , the scattered electric field $\mathbf{E}_s^v(x_m, y_m)$ satisfies the following relation representing the "data equation":

$$\mathbf{E}_s^v(X_m) = k_0^2 \iint_D g(X_m, X'_m) q(X') E^v(X') dx' dy', \quad (X_m) \in S, \quad (5)$$

The solution of the forward problem is carried out by the method of moment using pulse-basis function and point matching technique [17]. In order to validate the direct problem model obtained by using the method of moments (MoM), we compare the synthetic data with the experimental data given by [17]. We consider a single circular dielectric cylinder with a diameter of $d = 30$ mm and a relative permittivity of $\varepsilon_r = 3$. Time harmonic multi-frequency data are measured at 49 receiver positions on a circle with a radius of 760 mm and for different 36 emitter positions on a circle with a radius of 720 mm around the target. Relative to a fixed emitting antenna at 0° , the receiving antenna is rotated in a limited angular range from 60° to 300° with a 5° stepping ($M = 49$ positions) and the target is rotated in the full range from 0° to 350° with a 10° stepping. A frequency range from 1 GHz to 8 GHz with a 1 GHz stepping is used for the experimental data. A detailed description of the underlying experimental setup as well as the data sets is given in [17].

We assume that the unknown object is enclosed in a square investigation domain D of $150 \text{ mm} \times 150 \text{ mm}$ inside. The investigation domain is partitioned into 14×14 ($N = 196$) cells of equal size. Fig. 2 shows a comparison between the calculated and the measured fields. A considerable deviation is observed between measured data and those calculated by MoM. The difference can be the result of the noise introduced by the measurement system and the discretization of integral equations [8]. The quadratic relative error (QRE) between the measured data and those calculated by the forward model is about 30%. To improve the quality of the synthetic data, a white Gaussian noise with a SNR per sample of -10 dB is added to the computed data. The QRE is then reduced within 6%.

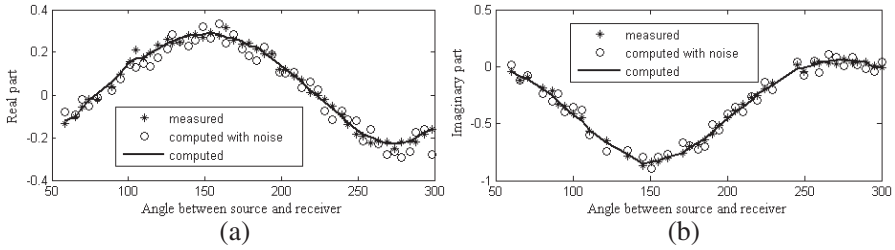


Figure 2. Comparison between the measured and computed scattered field (dielectric cylinder, $\epsilon_r = 3$, $f = 2$ GHz, $\phi_{inc} = 10^\circ$). (a) Real part. (b) Imaginary part.

3. A LEVEL SET METHOD FOR SHAPE RECONSTRUCTION

3.1. Inverse Scheme

Let Ω be a closed curve in $D \subset R^2$. Associated with Ω , we define $\phi(X) = \phi(x, y)$ as a signed distance function by:

$$\phi(X) = \begin{cases} \text{distance}(X, \Omega) & \text{if } X \in \Omega \\ -\text{distance}(X, \Omega) & \text{if } X \notin \Omega \end{cases} \quad (6)$$

It is clear that Ω is the zero level set of the function ϕ , Ω divide the domain D into two parts. The function is positive inside the object and negative outside.

Once the level set function is defined, we can use it to represent the contrast as a piecewise constant functions.

$$q(X) = \begin{cases} \epsilon_r - \epsilon_{ext}, & \text{if } \phi(X) > 0 \\ 0, & \text{if } \phi(X) < 0 \end{cases} = (\epsilon_r - \epsilon_{ext})H(\phi) = cH(\phi) \quad (7)$$

H is the Heaviside function. In order to identify the contrast function, we just need to identify the piecewise constant c and the level set function ϕ which reduce, and eventually minimize, the following cost functional:

$$J(q) = \sum_m \sum_v \|\mathbf{E}_{s,comp}^v(X_m) - \mathbf{E}_{s,mes}^v(X_m)\|^2 + \beta R(\phi) \quad (8)$$

where $\mathbf{E}_{s,mes}^v$ and $\mathbf{E}_{s,comp}^v$ design respectively the measured and computed electric fields at the observation points.

The length of level set curves $R(\phi) = \int_D |\nabla H(\phi)|$ is used as regularization term to prevent the zero level curves becoming oscillatory and to stabilize the reconstruction process.

The level set evolution can be described by the Hamilton-jacobi equation [17]:

$$\frac{\partial \phi}{\partial t} + F(X, t) \times \|\nabla \phi\| = 0 \quad (9)$$

We want to choose an evolution law $F(X)$ such that $\frac{dJ(q)}{dt}|_{t=0} \leq 0$, then $J(q)$ will decrease in the artificial time evolution during a sufficiently small time interval $[0 \ \tau]$.

We get by applying the chain rule [17] and using (9)

$$\frac{dJ(q)}{dt} = \frac{dJ(q)}{d\phi} \frac{d\phi}{dt} = - \left\langle \frac{dJ(q)}{d\phi}, F(X) \|\nabla \phi\| \right\rangle > \quad (10)$$

An obvious selection for $F(X)$ is

$$F(X) = \rho \frac{dJ(q)}{d\phi} \quad \text{with } \rho > 0 \quad (11)$$

We apply a gradient method to find the descent direction with respect to ϕ and the constant value q .

$$\frac{dJ(q)}{dc} = \int_D \frac{dJ}{dq} \frac{dq}{dc} dX = \int_D \frac{dJ}{dq} H(\phi) dX \quad (12)$$

$$\frac{dJ(q)}{d\phi} = \frac{dJ(q)}{dq} \frac{dq}{d\phi} + \beta \frac{dR(\phi)}{d\phi} = c\delta(\phi) \frac{dJ(q)}{dq} + \beta \frac{dR(\phi)}{d\phi} \quad (13)$$

So, we just need to compute the Gateaux derivative [17] $\frac{dJ(q)}{dq}$ and $\frac{dR(\phi)}{d\phi}$.

The differential of R with respect to ϕ is given by [10]:

$$\frac{dR(\phi)}{d\phi} = -\delta(\phi) \nabla \frac{\nabla \phi}{\|\nabla \phi\|} \quad (14)$$

The differential of J with respect to q is:

$$\frac{\partial J}{\partial q} = \sum_m \sum_v \left[\text{real}(\mathbf{E}_{s,\text{comp}}^v - \mathbf{E}_{s,\text{mes}}^v) \text{real} \frac{\partial \mathbf{E}_{s,\text{comp}}^v}{\partial q} + \text{imag}(\mathbf{E}_{s,\text{comp}}^v - \mathbf{E}_{s,\text{mes}}^v) \text{imag} \frac{\partial \mathbf{E}_{s,\text{comp}}^v}{\partial q} \right] \quad (15)$$

We use the Born approximation to compute $\frac{\partial \mathbf{E}_{s,\text{comp}}^v}{\partial q}$ and take the incident field in place of the total field as the driving field at each point in the object. The Equation (5) can be written as follows:

$$\mathbf{E}_s^v(X_m) = k_0^2 \int_D g(X_m, X'_m) q(X') \mathbf{E}_{inc}^v(X') dX' \quad (16)$$

So

$$\frac{\partial \mathbf{E}_{s,\text{comp}}^v(X_m)}{\partial q} = \overline{k_0^2 \times \mathbf{E}_{inc}^v \times g(X_m, X'_m)} \quad (17)$$

3.2. Algorithm

- Initialization: Choose initial level set function ϕ_0 and an initial contrast value q_0 .
- Calculate $\frac{dJ(q)}{dq}$.
- Choose a descent step α and update the contrast value c .

$$q_n = q_{n-1} - \alpha \times \int_D \frac{dJ}{dq} H(\phi) dX$$

- Choose $\rho > 0$ and calculate the evolution law

$$F(X) = \rho \frac{dJ(q)}{d\phi}$$

- Solve Equation (9) and update the level set function.
- Verify stopping criterion.

4. NUMERICAL EXPERIMENTS

In our numerical experiments, the data are generated by running the MoM forward modeling code on the correct permittivity distribution. Therefore, to make sure that the situations we model in our experiments are as realistic as possible, a Gaussian noise is added to the real and imaginary parts of the computed data. The physical domain is partitioned into 14×14 ($N = 196$) cells. The object is illuminated by an incident wave from 10 different directions and 16 measurements points are used for each incident angle. The scattered field is computed along a circle of radius 0.072 m around the object.

To quantify the reconstruction quality of the suggested methods, we define a mean quadratic relative error on the relative permittivity (MQREP) and on the scattered field (MQREF) as follows:

$$\text{MQREF} = \left(\frac{1}{MxV} \sum_m \sum_v \left\| \frac{E_{s,\text{comp}}^v(X_m) - E_{s,\text{mes}}^v(X_m)}{E_{s,\text{mes}}^v(X_m)} \right\|^2 \right)^{1/2} \quad (18)$$

$$\text{MQREP} = \left(\frac{1}{N} \sum_n \left\| \frac{\varepsilon_{r,n} - \varepsilon_{r,n}^*}{\varepsilon_{r,n}} \right\|^2 \right)^{1/2} \quad (19)$$

where ε_r and ε_r^* are the exact and computed values of the relative permittivity, respectively.

4.1. Two-identical Circular Cylinders

Our first numerical example tests whether the derived algorithm is able to reconstruct a relatively complicated shape where sources and receivers surround the area of interest. The geometry of this example is shown in Fig. 3(a).

The dielectric target is composed of two filled dielectric cylinders located in free space, with circular cross section of radius $a = 15$ mm and has a relative permittivity of $\epsilon_r = 2$.

Figure 3 shows that the deviation between boundaries of the reconstructed domain and dielectric target decreases as the algorithm progress. It is also shown that at the end of the optimization process, the shape of the cylindrical object is well detected and the MQREF is less than 02% (Fig. 4). Furthermore, the proposed scheme can handle topological changes in an automatic way, which allows the reconstruction of multiple objects using a single initial guess.

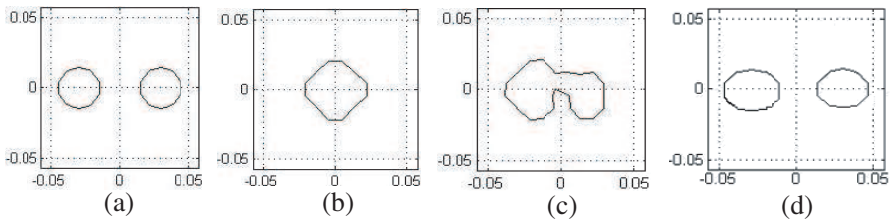


Figure 3. Reconstruction of two circular cylinders. (a) Original object. (b) Starting guess. (c) Reconstruction after 150 iterations. (d) Final reconstruction after 600 iterations.

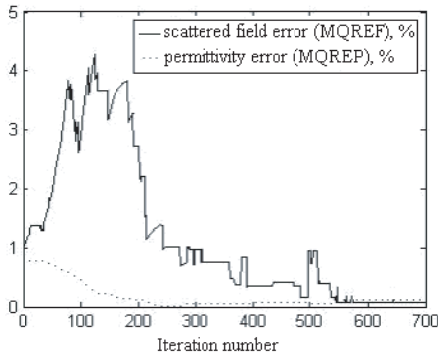


Figure 4. MQREF and MQREP as function of iteration number.

4.2. Circular Dielectric Cylinder with Hole

In our second numerical example, we consider a dielectric target shown in Fig. 5. Notice that an interesting feature of this geometry is the ‘hole’ in the body of the object, which is difficult to reconstruct.

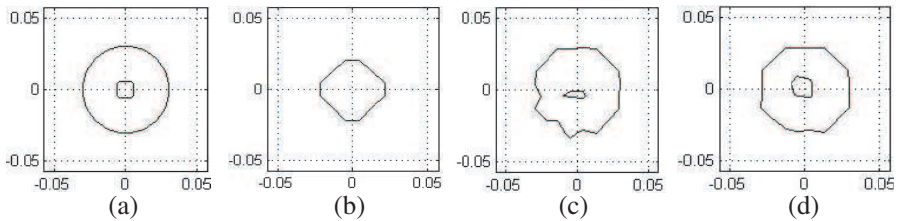


Figure 5. Reconstruction of circular dielectric cylinder with hole. (a) Original object. (b) Starting guess. (c) Reconstruction after 100 iterations. (d) Final reconstruction after 200 iterations.

Figure 5 shows that the proposed shape reconstruction algorithm using level sets is able to split and merge boundaries easily. In addition, the retrieved permittivity is very accurate and the cost function is almost zero after 250 iterations.

5. CONCLUSION

We have proposed a new scheme for the reconstruction of dielectric permittivity profile from scattered field data. In our research, we considered the situation where both the shapes and the permittivity values inside the object have to be recovered from the given data.

We use a level set method as a numerical tool to deform and construct the permittivity profile of the object. A gradient technique has been developed for finding evolution laws for the level set function which simultaneously reduce the least squares data misfit cost functional. A regularization term is added to the cost functional for a stable and efficient solution of the shape reconstruction problem.

Numerical experiments have been presented which demonstrate that the proposed scheme performs good reconstruction permittivity profile, even for complicated shape.

REFERENCES

1. Fang, Q., P. M. Meaney, and K. D. Paulsen, "Viable three-dimensional medical microwave tomography: Theory and numerical experiments," *IEEE Trans. on Antennas and Propagation*, Vol. 58, No. 2, 449–458, Feb. 2010.
2. Shea, J. D., P. Kosmas, S. C. Hagness, and B. D. Van Veen, "Three-dimensional microwave imaging of realistic numerical breast phantoms via a multiple-frequency inverse scattering technique," *Phys. Med. Biol.*, Vol. 37, No. 8, 4210–26, Aug. 2010.
3. Cao, C., L. Nie, C. Lou, and D. Xing, "The feasibility of using microwave-induced thermoacoustic tomography for detection and evaluation of renal calculi," *Phys. Med. Biol.*, Vol. 55, No. 17, 5203–12, Sep. 2010.
4. Yedlin, M. J., A. Cresp, C. Pichot, I. Aliferis, J. Y. Dauvignac, and S. Gaffet, "Ultra-wideband microwave imaging of heterogeneities," *Journal of Applied Geophysics*, Vol. 68, No. 1, 17–25, May 2009.
5. Remis, R. F. and P. M. Van den Berg, "On the equivalence of the Newton-Kantorovich and distorted Born methods," *Inverse Problems*, Vol. 16 2000, PII: S0266-5611(00)08356-8.
6. Joachimowicz, N., J. J. Mallorqui, J. C. Bolomey, and A. Broquetas, "Convergence and stability assessment of newton-kantorovich reconstruction algorithms for microwave tomography," *IEEE Trans. on Medical Imaging*, Vol. 17, No. 4, 562–570, Aug. 1998.
7. Omrogbe, D. E. A. and A. A. Osagiede, "Preconditioning the modified conjugate gradient method," *Global Journal of Mathematical Sciences*, Vol. 8, No. 2, 2009.
8. Mhamdi, B., K. Grayaa, and T. Aguilu, "Microwave imaging of dielectric cylinders from experimental scattering data based on the genetic algorithms, neural networks and a hybrid micro genetic algorithm with conjugate gradient," *Int. J. of Electron. Commun. (AEU)*, Vol. 65, No. 2, 140–147, Feb. 2011.
9. Mhamdi, B., K. Grayaa, and T. Aguilu, "Hybrid of particle swarm optimization, simulated annealing and tabu search for the reconstruction of two-dimensional targets from laboratory-controlled data," *Progress In Electromagnetics Research B*, Vol. 28, 1–18, 2011.
10. Osher, S. and J. Sethian, "Fronts propagation with curvature dependent speed: algorithms based on Hamilton–Jacobi formulations," *J. Comput. Phys.*, Vol. 79, No. 1, 12–49, 1988.
11. Chunming, L., X. Chenyang, G. Changfeng, and D. F. Martin, "Distance regularized level set evolution and its application to

- image segmentation,” *IEEE Trans. on Image Processing*, Vol. 19, No. 12, 3243–3253, Dec. 2010.
12. Brodersen, A., K. Museth, S. Porumbescu, and B. Budge, “Geometric Texturing Using Level Sets,” *IEEE Trans. on Visualization and Computer Graphics*, Vol. 14, No. 2, 277–288, Mar.–Apr. 2008.
 13. Young, S. K., K. B. Jin, and P. Il Han, “A level set method for shape optimization of electromagnetic systems,” *IEEE Trans. on Magnetics*, Vol. 45, No. 3, 1466–1469, Mar. 2009.
 14. Woten, D. A., M. R. Hajihashemi, A. M. Hassan, and M. El-Shenawee, “Experimental microwave validation of level set reconstruction algorithm,” *IEEE Trans. on Antennas and Propagation*, Vol. 58, No. 1, 230–233, Jan. 2010.
 15. Hu, J.-L., Z. Wu, H. McCann, L. E. Davis, and C.-G. Xie, “Quasi-three-dimensional method of moments for analyzing electromagnetic wave scattering in microwave tomography systems,” *IEEE Sensors Journal*, Vol. 5, No. 2, 216–223, Apr. 2005.
 16. Belkebir, K. and M. Saillard, “Special section: Testing inversion algorithms against experimental data,” *Inverse Problems*, Vol. 17, 1565–1571, 2001.
 17. Osher, S. and R. Fedkiw, “Level set methods and dynamic implicit surface,” *Applied Mathematical Sciences*, Vol. 53, Springer-Verlag, New York, 2003.